STRUCTURAL AND MAGNETIC PROPERTIES OF Co-Nd SUBSTITUTED $ZnFe_2O_4$ FERRITES SYNTHESIZED BY CO-PRECIPITATION TECHNIQUE

M. HUSSAIN[a,b*], M. UL-ISLAM[a], T. MEYDAN[b], Y. MELIKHOV[b], M. I. ARSHAD[c], G. MURTAZA[a], G. MUSTAFA[a]
[a]*Department of Physics, Bahauddin Zakariya University, Multan 60800, Pakistan*
[b]*Wolfson Centre for Magnetics, School of Engineering, Cardiff University,Cardiff, UK*
[c]*Department of Physics, G.C University Faisalabad, 38000, Pakistan*

A series of $Zn_{1-x}Co_xNd_yFe_{2-y}O_4$ spinel ferrites (x=0,0-0.5, y=0.00-0.10) was synthesized using the co-precipitation method sintered at 1000^{o}C. Synthesized Ferrites were characterized by x-ray diffraction (XRD), scanning electron microscopy (SEM) and vibrating sample magnetometery (VSM). The diffraction patterns show the formation of the spinel phase along with some traces of second phase Nd_2O_3. The lattice constant decreases with increasing Co-Nd ions because of the solubility of Nd^{3+} into the spinel lattice. SEM shows the decrease of the grain size with the increase of Co-Nd contents due to the fact that the second phase inhibits the growth of grain. VSM results show increasing trends of remanence and saturation magnetization due to the strengthening of the A-B sublattice interactions. The coercivity shows an increasing behaviour with the increase of co-substitutent contents.

(Received December 31, 2016; Accepted April 12, 2017)

Keywords: Spinel ferrites, saturation magnetization, remanence, coerecivity.

1. Introduction

Ferrimagnetic materials have been a focus of research during the last few decades due to their widespread applications in various industrial, biomedical, technological and defense applications. The properties of ferrites can be tailored using appropriate dopant for applications [1-8]. Many researchers have reported the substitution of elements in spinel ferrites ($ZnFe_2O_4$) for different applications [9-13]. Spinel Ferrites can be synthesized by various methods and amongst these, the most common are co-precipitation, hydrothermal, combustion, micro-emulsion, polymer-pyrolysis and sol-gel [14-19]. The co-precipitation technique offers several advantages over the others including processing at low temperature and/or better homogeneity, fine particle size etc. Co-substitution can also be easily achieved by the co-precipitation technique[11]. Similarly, it was earlier reported that rare earth element like Neodymium can affect the magnetic properties of the material [20-23] . In the present case Co-Nd substituted Zn-ferrites ($Zn_{1-x}Co_xNd_yFe_{2-y}O_4$) samples are prepared by the co-precipitation technique with the overall aim of improving the magnetic properties for different potential applications.

2. Materials and Methods

2.1. Sample Preparation

Spinel ferrites with general formula $Zn_{1-x}Co_xNd_yFe_{2-y}O_4$ (x=0.0-0.5, y=0.00-0.10) were prepared by co-precipitation technique with the following analytical grade reagents:$CoCl_2.6H_2O$,

*Corresponding authors: mudassarhussain@bzu.edu.pk

$Zn(NO_3)_2.6H_2O$, Nd_2O_3 and $Fe(NO_3)_3.9H_2O$.The precursor materials were dissolved in de-ionized water in desired stoichiometric proportions using an ultrasonic cleaner, subsequently stirred using a magnetic stirrer on hot plate at 60°C. The pH of the solution was adjusted in the range 10-11 using ammonia solution. The beaker containing the precipitates along with the solution was kept in a preheated water bath at 80°C for 90 min., under the ambient atmosphere. The precipitates were filtered, washed several times with deionized water to remove impurities and dried at 100°C for 12 h in an oven. The dried powder was ground in an agate mortar and pestle to obtain fine powder. The fine powder was pelletized under a pressure of 30 kN. Finally, the ferrite powder and the pellets were sintered at 1000°C for 6h in a muffle furnace.

2.2. Characterization of the samples

The x-ray diffraction (XRD) patterns of the powdered samples were obtained at room temperature using Philips Xpert PANalytical diffractometer operating at 30 mA and 40 kV. The surface morphology and elemental investigation was performed by JSM-6490 JEOL scanning electron microscope (SEM) equipped with energy-dispersive X-ray (EDX) spectroscopy. The magnetization hysteresis loops were recorded at room temperature using vibrating sample magnetometer (VSM, model Lake Shore 735).

3. Results and discussion

3.1. Structural Analysis

Fig.1 shows the XRD patterns of $Zn_{1-x}Co_xNd_yFe_{2-y}O_4$ (x=0.0-0.5, y=0.00-0.10)ferrites. It is evident that all the samples exhibit cubic spinel structure as a major phase and Nd_2O_3 as a secondary phase (denoted by asterisk in the XRD patterns). The secondary phase on the grain boundaries may be attributed to the high reactivity of Fe^{3+} with Nd^{3+} and limited solubility of Nd^{3+} into the spinel lattice [24, 25] .

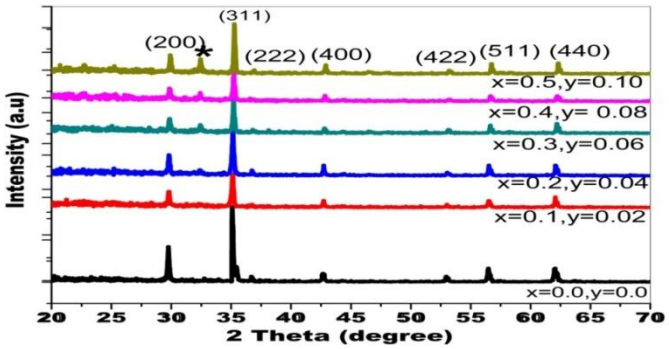

Fig. 1.XRD patterns of $Zn_{1-x}Co_xNd_yFe_{2-y}O_4$ ferrites (x=0.0-0.5, y=0.00-0.10)

The lattice constant decreases with increase in Co-Nd content. First explanation of the decrease in the lattice constant is due to the replacement of Fe^{3+} ions with Nd^{3+} ions. Instead of occupying the tetrahedral and the octahedral sites, Nd^{3+} segregate on the grain boundaries as reflected in the XRD results [25-27]. With further increase in the Nd^{3+}content, the aggregates at grain boundaries increase resulting in the further compression of the spinel lattice [27-29].

Table 1. Lattice constant (a), Unit cell volume (V) and Grain size of $Zn_{1-x}Co_xNd_yFe_{2-y}O_4$ ferrites (x = 0.0-0.5, y = 0.00-0.10)

Parameters	(x , y) (0 , 0)	(x , y) (0.1, .02)	(x , y) (0.2, 0.04)	(x , y) (0.3 , 0.06)	(x , y) (0.4, 0.08)	(x , y) (0.5, 0.10)
Lattice constant a (Å)	8.480	8.475	8.470	8.457	8.452	8.444
Unit Cell Volume V ($Å^3$)	611.28	608.85	607.72	604.90	603.74	602.04
Grain size (μm)	0.76	0.48	0.36	0.33	0.29	0,26

The second explanation for the decrease in the lattice constant is due to the replacement of Zn^{2+} with Co^{2+} since ionic size of Co^{2+} (0.78 A) is lower than that of Zn^{2+} (0.82 A) which has been reported earlier [30]. The values of unit cell volume of the samples are listed in Table 1.

3.2. Scanning Electron Microscopy (SEM) Analysis:

Scanning electron microscopy was used to examine the morphology and grain size of the investigated samples. Figure 2 shows the SEM profiles of few representative samples. It is evident from the micrographs that the materials are fine grained and the particle sizes are uniformly distributed. Grain size of these samples was also estimated by using line intercept method [23, 31].

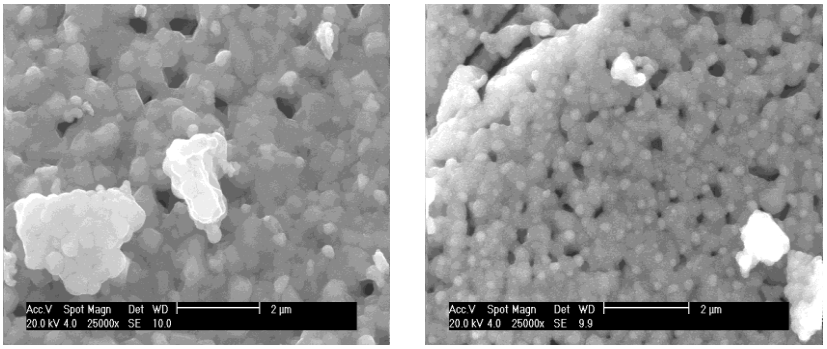

Fig. 2. SEM micrographs of $Zn_{1-x}Co_xNd_yFe_{2-y}O_4$ ferrites(x=0.1, y=0.02), (x=0.5, y= 0.10),

The average grain size decreases in the range of 0.76μm to 0.26μm depending Co-Nd substitution (Table 1). Since it is also evident that grain size decrease as Nd^{+3} content increases in the spinel lattice which may be attributed to the mobility of the grain boundaries. The close proximity of the Nd^{+3} ions potentially hinder grain boundary movement. Therefore, the grain size decreases with increasing Nd^{+3} content[23-24, 29,32].

3.3. Quantitative analysis (EDX)

Fig. 3 shows the energy dispersive X-ray (EDX) spectra of few representative samples. Analysis of spectra confirmed the presence of elements used for synthesize these materials and quantitative estimation of these elements in materials are listed in Table 2.

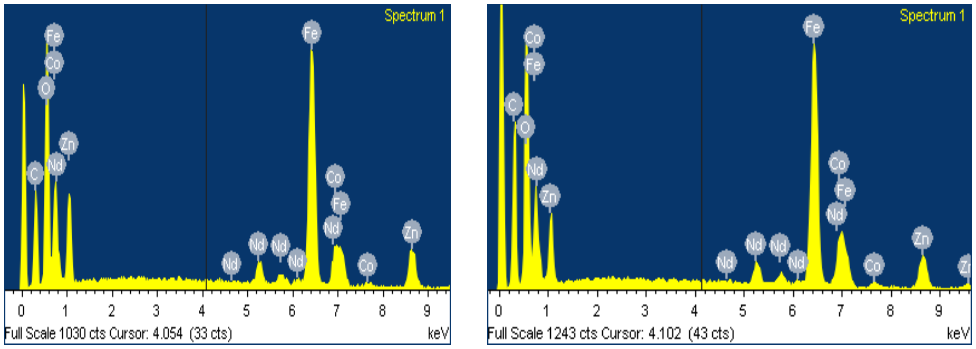

Fig. 3.EDX spectrum of $Zn_{1-x}Co_xNd_yFe_{2-y}O_4$ ferrites(x=0.2,y= 0.04) and (x=0.4,y=0.08)

Table 2.EDXS analysis of $Zn_{1-x}Co_xNd_yFe_{2-y}O_4$ferrites

Parameters	(x , y) (0 , 0)	(x , y) (0.1, 0.02)	(x , y) (0.2, 0.04)	(x , y) (0.3 , 0.06)	(x , y) (0.4 , 0.08)	(x , y) (0.5 , 0.10)
Zn (weight %)	27.15	24.45	21.64	18.85	16.09	13.34
Co (weight %)	-	2.40	4.82	7.21	9.58	11.92
Nd (weight %)	-	1.16	2.35	3.52	4.69	5.84
Fe (weight %)	46.33	45.60	44.93	44.27	43.62	42.98
O (weight %)	26.52	26.39	26.26	26.15	26.02	25.92
	100	100	100	100	100	100

3.4.Magnetic properties

Fig.4 shows the M-H loops of $Zn_{1-x}Co_xNd_yFe_{2-y}O_4$ (x=0.0-0.5, y=0.00 to 0.10) ferrites with the maximum applied field 18 kOe. Saturation magnetization and remanence both increases from 4.2 to 34.72 emu/g and 0.009 to 3.49 emu/g respectively with increasing Co-Nd contents, that is in agreement with previously reported results [23, 27]. The saturation magnetization increases due to strong A-B-interactions. Zn^{2+} ions occupy tetrahedral-sites while Co^{2+} and Nd^{3+} ions have a tendency to occupy the octahedral sites [9, 18, 23, 29, 33,34]. It is observed that replacement of Fe^{3+} ions with Nd^{3+} ions causes an increase in saturation magnetization as reported earlier [23, 24, 27]. The second reason for the increase of both saturation magnetization and coercivity is due to replacement of Zn^{2+} with Co^{2+}. As Zn^{2+} ions are replaced with Co^{2+} ions in the lattice, the saturation magnetization and the coercivity increase is due to the anisotropic nature of Co^{2+} as previously reported [9]. The ratio of remanence to saturation magnetization (Mr/Ms) lies in the range 0.00-0.33, well below of typical value 1 [35]. In the present case it has been assumed that the particles consist of single domain magnetic structures. Figure 4 reveals an increasing trend of coercive field with increasing Co-Nd contents [29]. However it has been observed that the coercivity increases in the range 21.7-72.26 Oe [9]. The factors that influence the coercivity include morphology, magnetocrystalline anisotropy, the domain sizes etc [36]. With increase in the substitution of Neodymium, the surplus Nd^{3+}ions form a secondary phase. The motion of the magnetic domain walls is hindered due to the secondary phase that is located at the grain boundary and it also induces distortion within the grains that result in the initiation of the internal stresses. Moreover, when Nd^{3+} ions increase in the spinel lattice, the spin-orbit coupling strength also increases, and thus the magnetic anisotropy is eventually enhanced. The coercivity and the anisotropy are directly linked, and as a result, the coercivity increases with increase of Co-Nd substitution [24, 29].

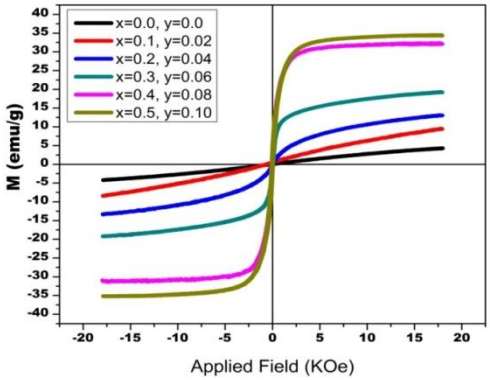

Fig. 4. M-H Loops of co-substituted $Zn_{1-x}Co_xNd_yFe_{2-y}O_4$ ferrites (x=0.0-0.5, y=0.00-0.10)

Table 3. Saturation Magnetization (Ms), Remanence, (Mr), Coercivity (Hc), Squareness ratio (Mr/Ms) of $Zn_{1-x}Co_xNd_yFe_{2-y}O_4$ferrites (x=0.0-0.5, y=0.00-0.10)

Parameters	(x, y) (0, 0)	(x, y) (0.1, 0.02)	(x , y) (0.2, 0.04)	(x , y) (0.3, 0.06)	(x , y) (0.4, 0.08)	(x, y) (0.5, 0.10)
Saturation Magnetization, Ms (emu/g)	4.20	8.82	12.8	19.1	31.62	34.72
Remanence, Mr (emu/g)	0.009	0.0479	0.2449	0.9624	3.0720	3.4925
Coercivity, Hc	21.75	28.55	44.82	34.49	63.37	72.26
Squareness Ratio, Mr/Ms	-	0.005	0.019	0.05	0.09	0.10

4. Conclusions

The Co-Nd co-substituted ferrites were successfully synthesized by co-precipitation technique. The synthesized ferrites exhibit cubic spinel structure with appearance of a secondary Nd_2O_3 phase. XRD confirmed the spinel phase formation. Lattice constant decreases due to solubility limit of Nd^{+3} in the spinel lattice with increase in Co-Nd content.

SEM images shows decrease in grain size from 0.76 to 0.26μm with increase of Co-Nd contents. EDX spectra reveal the presence of all the constituent ions in the synthesized ferrites. The saturation magnetization increases with increase of Co-Nd contents due to the strengthening of A-B interactions. Coercivity of un-substituted Zn-ferrites is small and it increases with increasing Co-Nd co-substituted contents due to rise of magnetic anisotropy.

Acknowledgements

The authors are thankful to the Higher Education Commission (HEC) of Pakistan for the financial assistance under HEC International Research Support Initiative Program (IRSIP).

References

[1] A.R. Reddy, et al., Journal of materials science, **34**(13), 3169(1999).

[2] J.Kulikowski, Journal of Magnetism and Magnetic Materials, **41**(1-3), 56(1984).
[3] A.Goldman, Modern ferrite technology. 2006: Springer Science & Business Media.
[4] Y.Köseoğlu, et al., Polyhedron, **28**(14), 2887(2009).
[5] R. Bhowmik, R. Ranganathan, Journal of alloys and compounds**326**(1),128(2001).
[6] N. Sharma, et al., Journal of Magnetism and Magnetic Materials **369,** 162(2014).
[7] S. Algude, et al., Jo of Magnetism and Magnetic Materials **350,** 39(2014).
[8] S. Amiri, H. Shokrollahi, Journal of Magnetism and Magnetic Materials **345,** 18(2013).
[9] X.Huang, et al., Journal of Alloys and Compounds **627,** 367(2015).
[10] Y.Liu, et al., Journal of Magnetism and Magnetic Materials**349**, 57(2014).
[11] J. Xie, et al., Journal of magnetism and magnetic materials **314**(1), 37(2007).
[12] M.C.Dimri, et al., Journal of electroceramics **16**(4), 331(2006).
[13] S. Mahmud, et al., Journal of Magnetism and Magnetic Materials **305**(1), 269(2006).
[14] D. R.Cornejo, A. Medina-Boudri, J. Matutes-Aquino, Physica B: Condensed Matter **320**(1), 270(2002).
[15] X.Yi, et al., Materials Science and Engineering: B **34**(1), L1-L3(1995).
[16] K. C. Patil, S.T. Aruna, T. Mimani, Current Opinion in Solid State and Materials Science, **6**(6), 507 (2002).
[17] V. Pillai, D. Shah, Journal of Magnetism and Magnetic Materials **163**(1), 243 1996.
[18] X.-M. Liu, et al., Physica B: Condensed Matter **370**(1), 14(2005).
[19] W.C. Kim, et al., Journal of magnetism and Magnetic materials **215,** 217(2000).
[20] E. Pervaiz, I. Gul. Influence of rare earth (Gd3+) on structural, gigahertz dielectric and magnetic studies of cobalt ferrite. in Journal of Physics: Conference Series. 2013. IOP Publishing.
[21] Q.Lin, et al. Journal of Nanomaterials, **2015,** 8(2015).
[22] M. T. Rahman, M. Vargas, C. Ramana, Journal of Alloys and Compounds **617,** 547(2014).
[23] T.Shinde, A. Gadkari, P. Vasambekar, Journal of Materials Science: Materials in Electronics, **21**(2), 120(2010).
[24] I.Ahmad,et al., Journal of Electronic Materials, **44**(7), 2221(2015).
[25] L.Zhao, et al., Materials Letters**60**(1), 104(2006).
[26] M. Ahmed, E. Ateia, S. El-Dek, Materials Letters, **57**(26), 4256(2003).
[27] M. Eltabey, W. Agami, H. Mohsen, Journal of advanced research, **5**(5), 601(2014).
[28] M.A.Iqbal, et al., Ceramics International, **39**(2), 1539(2013).
[29] M.A.Iqbal, et al., Journal of Alloys and Compounds, **579,** 181(2013).
[30] S.Nasrin, et al., IOSR Journal of Applied Physics **6**(2), 58(2014).
[31] M. Ahmad, et al., Current Applied Physics, **12**(6), 1413(2012).
[32] M.Ahmad, et al., Ceramics International **37**(8), 3691(2011).
[33] G.Sathishkumar, C. Venkataraju, K. Sivakumar, Materials Sciences and Applications **1**(01), 19 (2010).
[34] L.B.Tahar, et al., Materials Research Bulletin **42**(11), 1888(2007).
[35] D.S.Mathew, R.-S. Juang, Chemical Engineering Journal, **129**(1), 51(2007).
[36] G. Mustafa, et al., Journal of Magnetism and Magnetic Materials**378,** 409(2015).